Supplementary Information

Exploration of conjugated π-bridge units in *N,N*-bis(4-methoxyphenyl)naphthalen-2-amine derivative-based hole transporting materials for perovskite solar cell applications: a DFT and experimental investigation

Puhang Cheng[‡], Qian Chen[‡], Hongyuan Liu, Xiaorui Liu[*]

Key Laboratory of Luminescence Analysis and Molecular Sensing, Ministry of Education, School of Chemistry and Chemical Engineering, Southwest University, Chongqing 400715, P.R. China

[‡]*The authors contribute equally to this work.*

[*]*Corresponding authors: Xiaorui Liu; E-mail addresses: liuxiaorui@swu.edu.cn (X. Liu)*

Contents:

1. Computational Details

In order to choose a suitable method (which is accordance with the experiment value), we tested a series of functional, including HSE, B3LYP, B3P86, BMK and PBE0, to optimize the ground-state (S_0) geometry of investigated model compound H101, CP1 and CP2 using the 6-311G(d,p) basis set (Table S1). As shown in Table S1, the results indicate that the HOMO and LUMO energy level of H101 (-5.07 eV, -2.37 eV) computed at B3P86/6-311G(d,p) level agree with the experiment value (-5.18 eV, -2.48 eV) very well. So, we optimize the S_0 geometry of investigated molecules CP1 and CP2 using the B3P86/6-311G(d,p) method and basis set.[1] The energies of all of the obtained geometries are ensured to be the lowest because the optimized structures do not exhibit imaginary frequency.

The optical absorptions of all HTMs were simulated by TD-DFT with the BMK/6-31G(d) levels in dichloromethane solution with a polarizable continuum model (PCM). [2, 3] Compared with the experimental value (404 nm) of arylamine derivatives-based HTM (H101), using the TD-BMK/6-31G(d) method in dichloromethane solution can yield an accurate absorption peak at 398 nm. Moreover, energy calculations, including electron affinities, adiabatic ionization potential and absolute hardness of the investigated systems, were performed using the B3P86/6-311G(d,p) method. The solvation free energy for all molecules were calculated using the TD-BMK/6-31G(d) method in chlorobenzene solution or in gas. The calculations of ground-state geometry, energy and optical absorptions on DFT and TD-DFT were carried out by the Gaussian 09 program.[4]

The charge mobility of the designed HTMs was calculated from the Einstein relation: [5, 6]

$$\mu = \frac{eW}{k_B T} \qquad \text{(S1)}$$

where e, W, k_B and T are the electron charge, the charge diffusion coefficient, Boltzmann constant and temperature (300 Kelvin), respectively. For a n-dimensional system, W is defined as the ratio between the mean-square

displacement and the diffusion time: [7]

$$W = \lim_{t\to\infty} \frac{1}{2n} \frac{\left\langle x(t)^2 \right\rangle}{t} \tag{S2}$$

For a spatially isotropic system, the homogeneous diffusion constant W can be approximately evaluated by: [8]

$$W = \frac{1}{2n} \sum_i r_i^2 k_i p_i \tag{S3}$$

where i runs over all nearest adjacent molecules. The parameters such as d, r_i, k_i and p_i are the spatial dimensionality, the hopping distance, charge transfer rate (k) and hopping probability ($p_i = k_i / \sum_i k_i$), respectively.

Here, The parameter of charge transfer rate (k) for organic molecules can be calculated from the Marcus–Hush equation:[6, 9, 10]

$$k = \frac{v^2}{h} \sqrt{\frac{4\pi^3}{\lambda k_B T}} \exp\left(\frac{-\lambda}{4 k_B T}\right) \tag{S4}$$

Where v, h and λ are the electronic coupling, Planck's constant, reorganization energy, respectively. It's reported that descriptions of the charge transfer on basis of the hopping mechanism was universally accepted. [11-13] In equation (5), the parameters such as λ and v are the key factors to determine the transfer rate of organic materials.

The inner reorganization energy λ_h for holes of HTMs could be calculated as follows:[14]

$$\lambda_h = E_+ - E_+^* + E^* - E \tag{S5}$$

where E represent the energy of the neutral segment and E_+^* is the cation segment. E_+ represent the energy of the neutral segment from the geometries of cation segment. E^* is the cation segment on basis of the neutral segment.[15] Energies of the neutral segment and the cation segment for inner reorganization energy of HTMs were performed using the LC-wPBE/6-311G(d,p) method and basis set.

The parameter of electronic coupling (v) could be obtained from the equation as shown below:[16, 17]

$$v = \frac{J - S(H_1 + H_2)/2}{1 - S^2} \tag{S6}$$

where S, J and H are the spatial overlap, charge transfer integral and site energies. The parameter of J could be

simulated by the equation as shown below:[16, 17]

$$J = \langle \varphi^1_{\mathrm{HOMO}} | h_{\mathrm{ks}} | \varphi^2_{\mathrm{HOMO}} \rangle \quad \text{(S7)}$$

where h_{ks} is the Kohn-Sham Hamiltonian between two fragments. The parameters such as $\varphi^1_{\mathrm{HOMO}}$ and $\varphi^2_{\mathrm{HOMO}}$ are the HOMOs of two fragments, respectively. The electronic coupling could be simulated from the PW91/TZP levels in ADF program.[18-21]

In order to calculate the parameter of electronic coupling for HTMs, it was compelled to obtain the dimer structure which was defined as adjacent segments from the crystal structures of molecules. The crystal structure of the investigated HTMs can be predicted from the polymorph module in Material Studio software. [22, 23] The geometry of the cluster models used in the present study was taken from the B3P86/6-311G(d,p) level. The Dreiding force field was used for the prediction.[24] For the investigated molecules, the polymorph calculations are restricted to the ten most probable space groups such as $P2_1/c$, $P1$, $P2_12_12_1$, $C2/c$, $P2_1$ and $Pbca$.[25] To verify the rationality of the selected models in this work, the H101 crystal structure was predicted using the same methods. On basis of the simulated results for the predicted H101 crystal structure, the calculated the hole mobility of 7.01×10^{-5} cm^2 V^{-1} s^{-1} is in good agree with that of experimental value (6.57×10^{-5}). [26]This validates that the calculation method is reasonable to a certain degree. Then, the crystal structures were sorted according to their total energy. On basis of the crystal structures, we selected a molecule as center. All of the adjacent fragments with the center are defined as the transport pathways. That is to say, each transport pathway is the paired dimer between neighboring and center molecules.

2. Experimental Section

2.1 Materials

In this work, all starting reagents and solvents were used as received from commercial sources and used as received unless specially stated. Including 2,6-dibromonaphthalene (95%), 2,7-dibromopyrene (95%), N,N-bis(4-

methoxyphenyl)-6-(4,4,5,5-tetramethyl-1,3,2-dioxaborolan-2-yl)naphthalen-2-amine (95%) . FAI, MABr, Indium tin oxide (ITO) coated glass, PbI_2 (99.999%), Spiro-OMeTAD (99.5%), CsI (99%) and $PbBr_2$ (99.999%) were purchased from Advanced Election Technology CO,.Ltd**.** PEDOT:PSS (Heraeus, Clevios PVP Al 4083) were purchased from *p*-OLED (China). Lithiumbis-(trifluoromethylsulfonyl)imide (LiTFSI, 99%) and 4-(tert-Butyl)pyridine (TBP, 99%) were purchased from *p*-OLED (China). Anhydrous DMSO (99.8%), DMF (99.8%) and chlorobenzene (99.8%) were purchased from Sigma Aldrich. Solvents for chemical synthesis such as DMF and DCM were treated according to the standard procedures.

2.2 Cyclovoltammetry (CV)

Cyclicvoltammetry was measured on a CHI760E Electrochemical Workstation equipped with a glass carbon working electrode, a platinum wire counter electrode, and an Ag/AgCl reference electrodes. The measurements were carried out in dry dichloromethane (DCM) with tetrabutylammonium hexafluorophosphate (0.1 mol L^{-1}) as the supporting electrolyte under a nitrogen atmosphere at a scan rate of 50 mV s^{-1}. The potential of Ag/AgCl reference electrode was internally calibrated by using the ferrocene/ferrocenium redox couple (Fc/Fc^+). According to the onset oxidation potential of the CV measurements, the highest occupied molecular orbital (HOMO) was estimated based on the vacuum energy level of ferrocene (5.1 eV): HOMO = – (Eonset – EFc/Fc+) – 5.1 eV.

2.3 Device Fabrication

Patterned FTO−TiO_2 glass were used as received from commercial sources (Advanced Election Technology CO,.Ltd). A perovskite precursor solution (1.30 M PbI2, 1.19 M FAI, 0.14 M PbBr2, 0.14 M MABr, and 0.07 M CsI in DMF:DMSO mixed solution with a v/v of 4:1) was spin-coated in a two-step program at 1000 and 6000 rpm for 10 and 30 s, respectively. During the second step, 150 μL of chlorobenzene was dropped on the spinning substrate at 15 s after the start-up. Next, the as-spun perovskite layer was annealed on a hot plate at 120 °C for 60 min to drive

off solvent and form the perovskite phase. The hole-transporting layers (HTLs) were deposited by spin-coating with 30 s (6000 rpm for H101, 3000 for CP1 and CP2) corresponding solution on top of perovskite films. The HTM solution was each prepared by dissolving H101 (72.5 mg) in 1 mL chlorobenzene, 28.8 mL tert-butylpyridine (TBP) solution and 17.5 mL lithium bis(trifluoro methylsulfonyl) imide (Li-TFSI)/acetonitrile (520 mg/1 mL). Different HTMs (CP1 and CP2) were all dissolved in chlorobenzene in a concentration of 30 mg mL^{-1}, with *t*BP and Li-TFSI as dopants. After oxidizing the HTM layers in air for 15 h, the devices were pumped to lower than 10^{-5} torr and an approximately 100 nm thick Ag counter electrode was deposited on top. The active area of our device is 0.06 cm^2.

2.4 Mobility Measurements

Hole-only devices are fabricated with the structure ITO/PEDOT:PSS/HTM/MoO_3/Ag. The dark *J–V* characteristics of hole-only devices were measured under N_2 atmosphere inside a glove box. PEDOT:PSS was deposited on the ITO substrate at 5000 rpm for 30 s, followed by annealing at 120 ºC for 30 min and the conditions of spin coating HTM are consistent with the Device fabrication. Mobility is extracted by fitting the current density-voltage curves using space charge limited current (SCLC). Fitting the results to a space charge limited form, based on the following equation $J = 9\varepsilon_\theta\varepsilon_\gamma\mu_h V^2/8L^3$. J is the current density, L is the film thickness of the active layer, μ_h is the hole mobility, ε_γ is the relative dielectric constant of the transport medium, ε_θ is the permittivity of free space (8.85×10^{-12} F m^{-1}), V is the internal voltage of the device.

2.5 Measurements

The nuclear magnetic resonance (NMR) spectra were obtained from a BRUKER AVANCE III 600 MHz NMR Instrument (in $CDCl_3$ or in DMSO). Mass spectra were collected on a Bruker impact II high-resolution mass spectrometer. MALDI-TOF HRMS was performed on a Bruker Autoflex instrument, using 1,8,9-trihydroxyanthracene as a matrix. UV-vis absorption spectra were measured on a Shimadzu UV-2450 absorption

spectrophotometer. The current–voltage (*J–V*) curves were measured under 100 mW cm^{-2} (AM 1.5 G) simulated sunlight using Keithley 2400 in conjunction with a Newport solar simulator (94043A). Use atomic force microscopy (AFM) to characterize the morphology, the model is CSPM5500A. Steady-state PL spectra were recorded on Fluorolog®-3 fluorescence spectrometer (Horiba). Time-resolved PL decay curves were measured by a single photon counting spectrometer from Horiba Instruments (Fluorolog®-3) with a Picosecond Pulsed UV-LASTER (LASTER375) as the excitation source.

3. Target molecule synthesis

N6,N6,N6'',N6''-tetrakis(4-methoxyphenyl)-[2,2':6',2''-ternaphthalene]-6,6''-diamine (CP1): The compound 1 (2,6-dibromonaphthalene, 0.1785 g, 0.6 mmol) and the compound 2 (N,N-bis(4-methoxyphenyl)-6-(4,4,5,5-tetramethyl-1,3,2-dioxaborolan-2-yl)naphthalen-2-amine, 0.7715 g, 1.6 mmol) were accurately weighed and put into the reaction flask, the catalyst $Pd(PPh_3)_4$ (0.076 g, 0.065 mmol) was added under a nitrogen atmosphere, the system was vacuum replaced three times, and the toluene (50 mL) and potassium carbonate solution(2M 20 ml) prepared by deoxygenation in advance were added. The reaction was refluxed at 110 ˚C overnight. Cool to room temperature, quench the reaction with water, dry with anhydrous sodium sulfate and extract the organic solvent with dichloromethane. The product was obtained as yellow powder by recrystallization method. (0.320 g, yield: 62%).^{1}H NMR (600 MHz, Chloroform-d) δ 8.09 (s, 2H), 8.00 (s, 2H), 7.93 (d, J = 8.5 Hz, 2H), 7.82 (dd, J = 8.5, 1.8 Hz, 2H), 7.70 (dd, J = 30.5, 8.7 Hz, 4H), 7.57 (s, 2H), 7.10 (d, J = 83.6 Hz, 12H), 6.80 (d, J = 8.3 Hz, 8H), 3.76 (s, 12H). ^{13}C NMR (151 MHz, Chloroform-*d*) δ 156.07, 138.50, 136.11, 133.82, 132.92, 129.37, 128.90, 128.70, 127.25, 126.65, 126.04, 125.93, 125.66, 125.32, 122.95, 114.77, 55.53. MS: m/z= 834.3457, calcd for $C_{58}H_{46}N_2O_4$: 835.02.

6,6'-(pyrene-2,7-diyl)bis(N,N-bis(4-methoxyphenyl)naphthalen-2-amine) (CP2): The compound 1 (2,7-

dibromopyrene, 0.2016 g, 0.56 mmol) and the compound 2 (N,N-bis(4-methoxyphenyl)-6-(4,4,5,5-tetramethyl-1,3,2-dioxaborolan-2-yl)naphthalen-2-amine, 0.7492 g, 1.6 mmol) were accurately weighed and put into the reaction flask, the catalyst $Pd(PPh_3)_4$ (0.068 g, 0.06 mmol) was added under a nitrogen atmosphere, the system was vacuum replaced three times, and the toluene (50 mL) and potassium carbonate solution(2M 20 ml) prepared by deoxygenation in advance were added. The reaction was refluxed at 110 ˚C overnight. Cool to room temperature, quench the reaction with water, dry with anhydrous sodium sulfate and extract the organic solvent with dichloromethane. The product was obtained by column chromatography (PE/EA = 5:1) as a yellow powder (0.270 g, yield: 53%).^{1}H NMR (600 MHz, DMSO-d6) δ 8.73 (d, J = 2.4 Hz, 4H), 8.42 (s, 2H), 8.34 – 8.27 (m, 4H), 8.10 – 8.04 (m, 2H), 7.91 (d, J = 8.8 Hz, 2H), 7.81 (d, J = 8.7 Hz, 2H), 7.16 (dd, J = 10.8, 2.3 Hz, 4H), 7.12 (dd, J = 8.7, 2.3 Hz, 8H), 6.97 (dd, J = 8.7, 2.4 Hz, 8H), 3.78 (d, J = 2.4 Hz, 12H). ^{13}C NMR (151 MHz, Chloroform-*d*) δ 156.07, 138.95, 136.53, 131.60, 129.46, 128.97, 127.95, 127.38, 126.68, 126.53, 126.41, 123.83, 123.75, 122.96, 114.79, 55.54. MS: m/z= 908.3614, calcd for $C_{64}H_{48}N_2O_4$: 909.10.

4. Experimental characterization

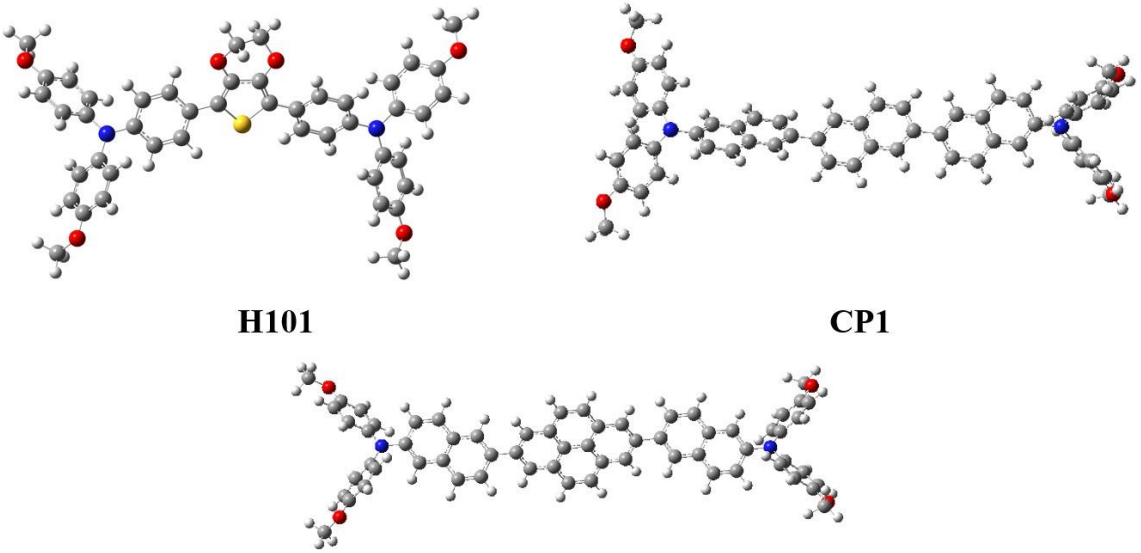

Fig. S1 Optimized structures for the hole transporting materials from B3P86/6-311G(d) calculations.

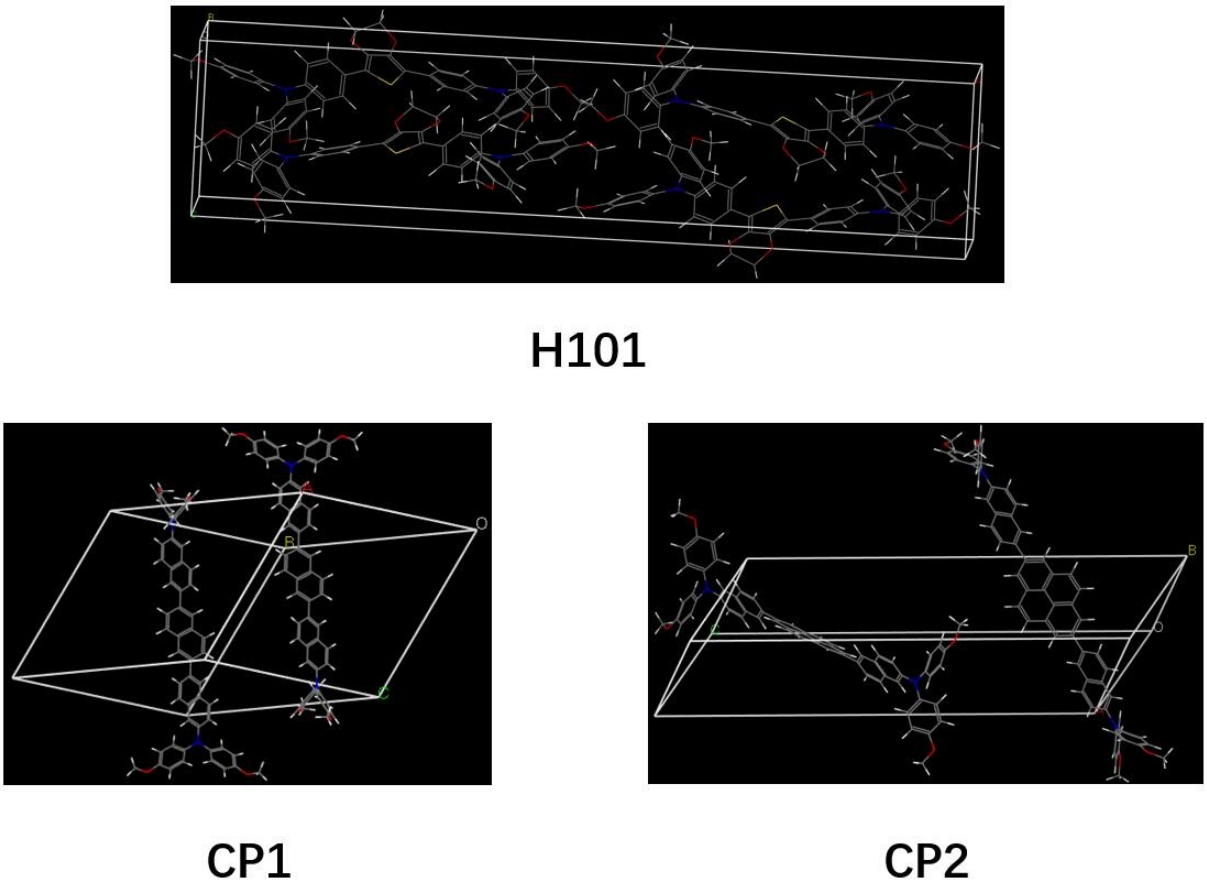

Fig. S2 Calculated crystal structures with the lowest total energies of the investigated molecules

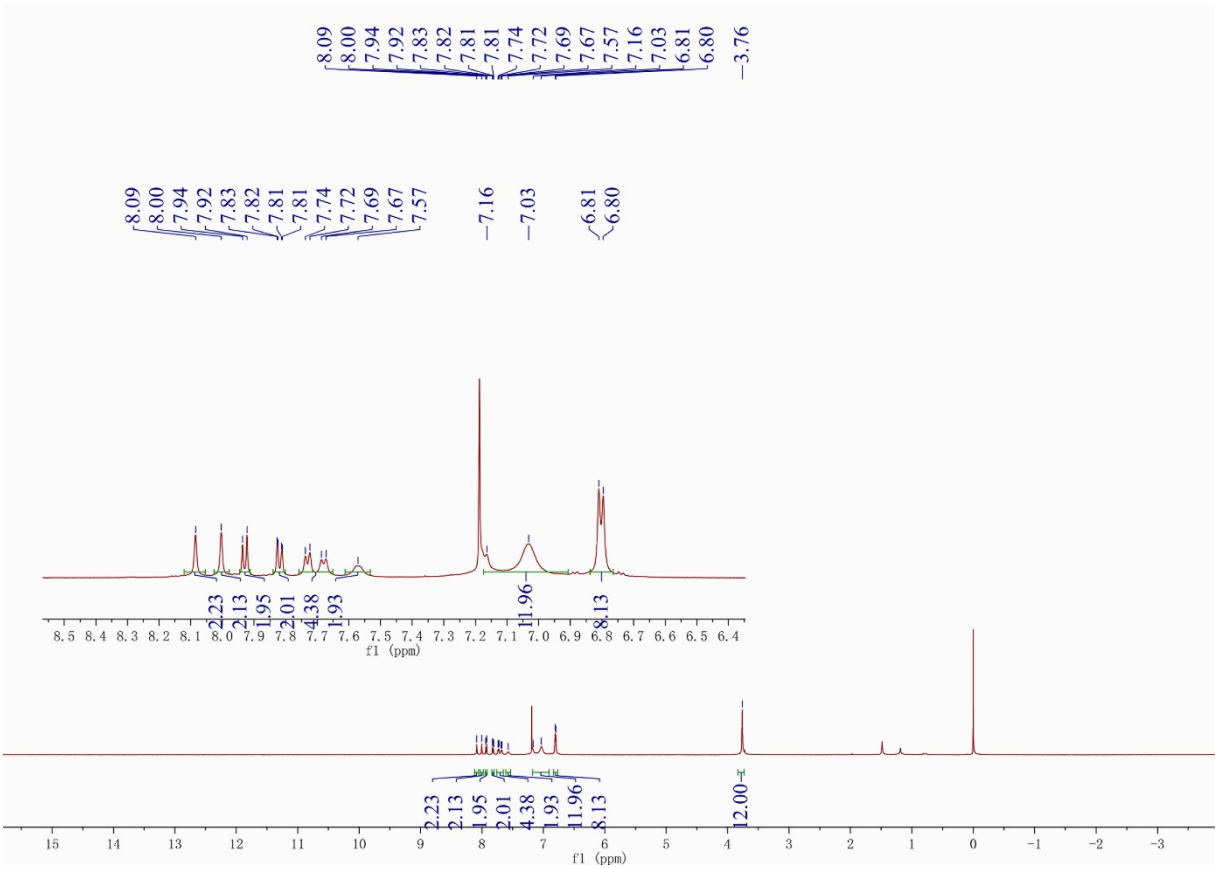

Fig. S3. The ^{1}H NMR spectrum of CP1

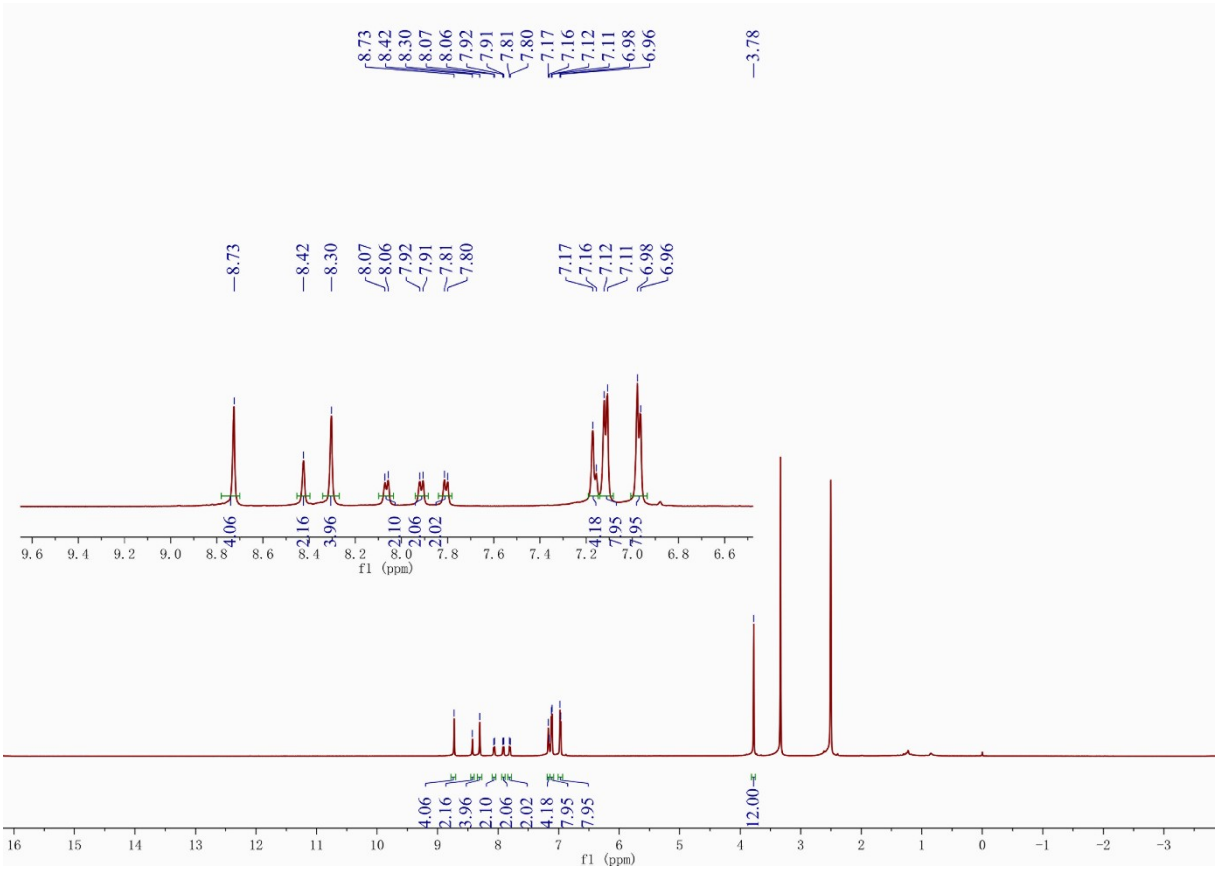

Fig. S4. The ^{1}H NMR spectrum of CP2

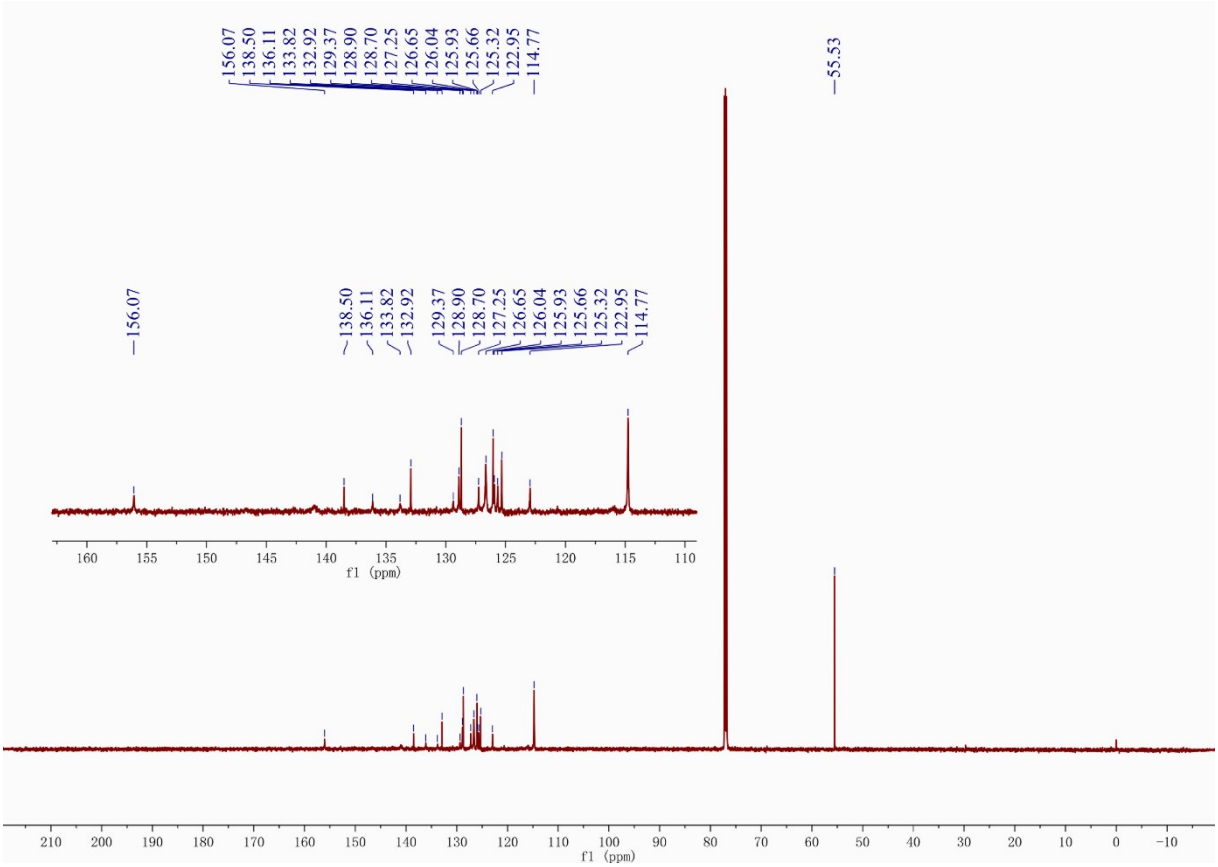

Fig. S5. The ^{13}C NMR spectrum of CP1

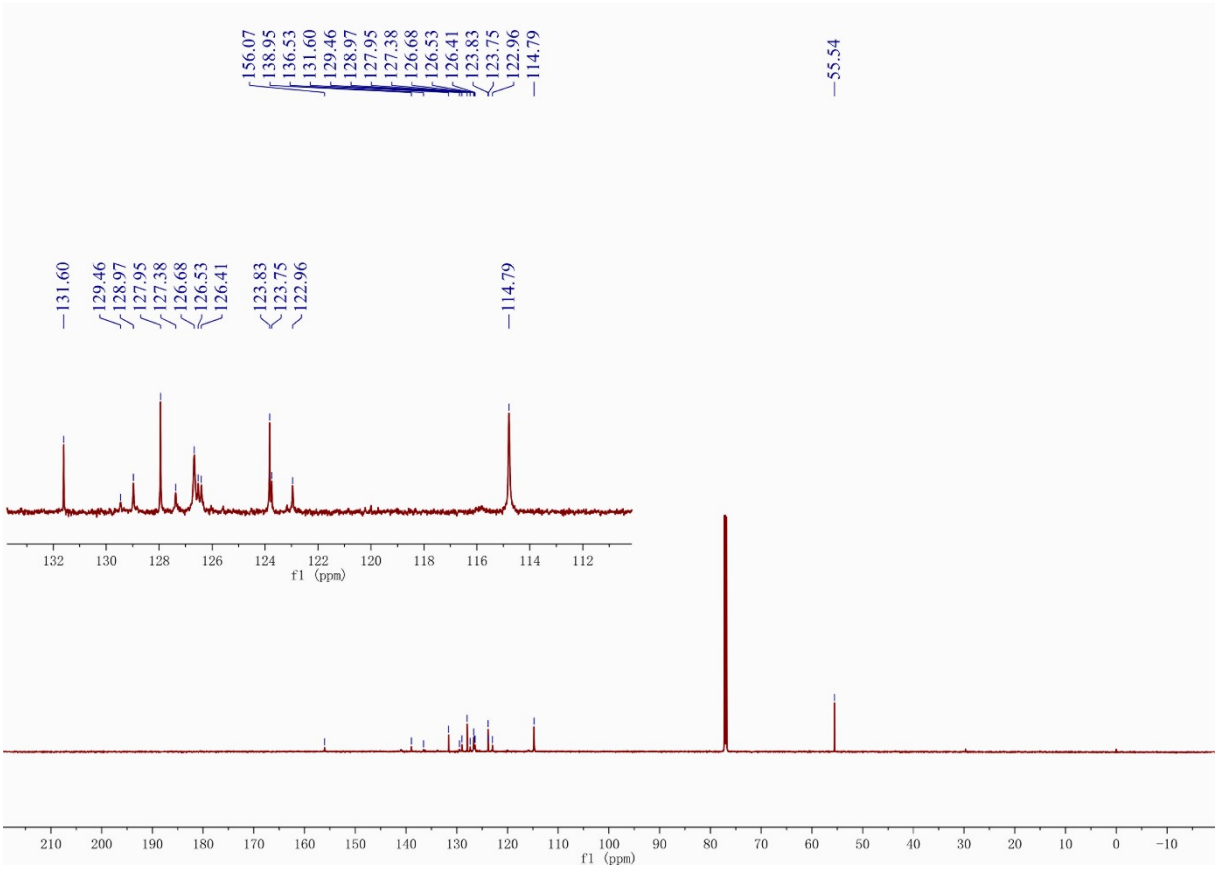

Fig. S6. The ^{13}C NMR spectrum of CP2

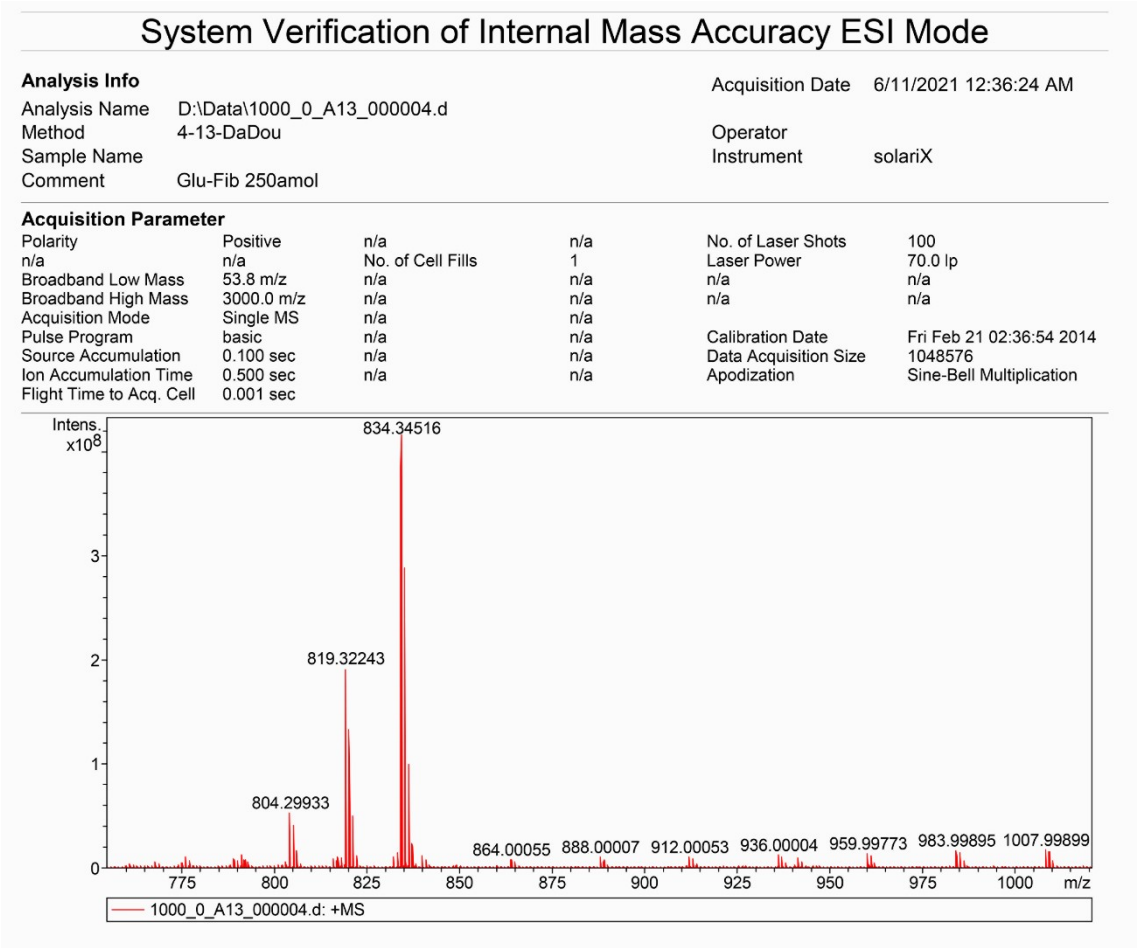

Fig. S7. Mass spectrometry of CP1

MASS SPECTROMETRY REPORT

Sample No.	Formula (M)	Measured m/z	Calc. m/z	Diff (ppm)
CP1	$C_{58}H_{46}N_2O_4$	834.3452	834.3457	0.60

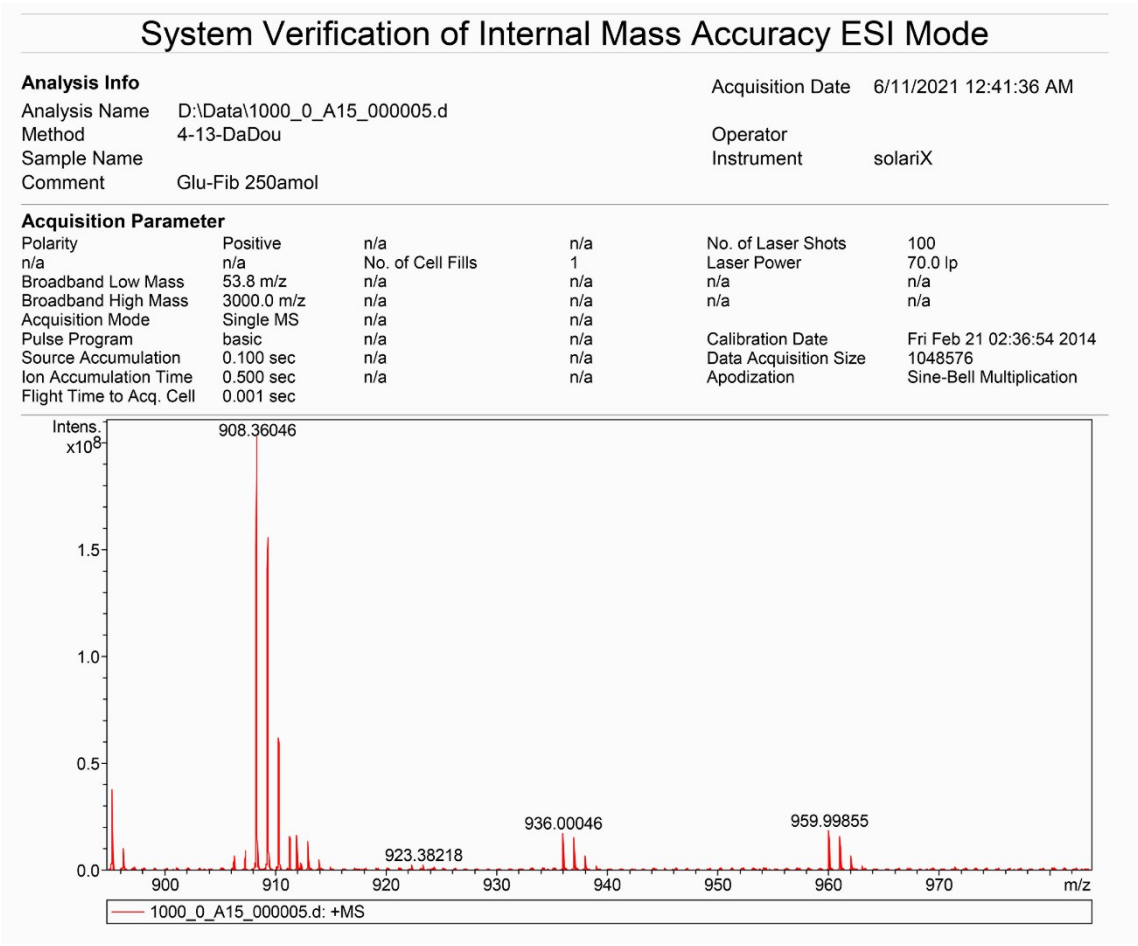

Fig. S8. Mass spectrometry of CP2

MASS SPECTROMETRY REPORT

Sample No.	Formula (M)	Measured m/z	Calc. m/z	Diff (ppm)
CP2	$C_{64}H_{48}N_2O_4$	908.3605	908.3614	0.99

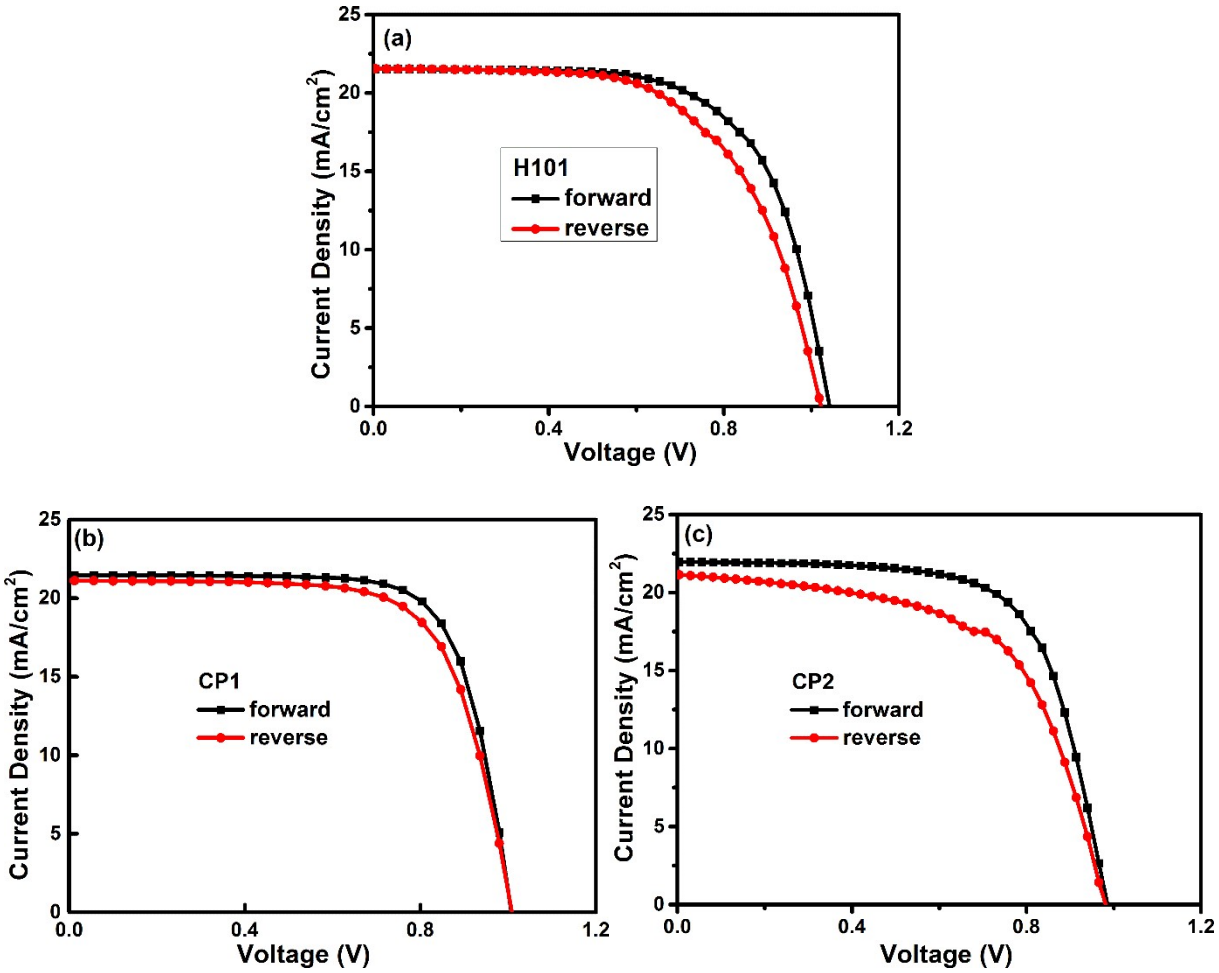

Fig. S9. *J–V* curves measured of devices under reverse and forward voltage scans with the HTMs H101, CP1 and CP2.

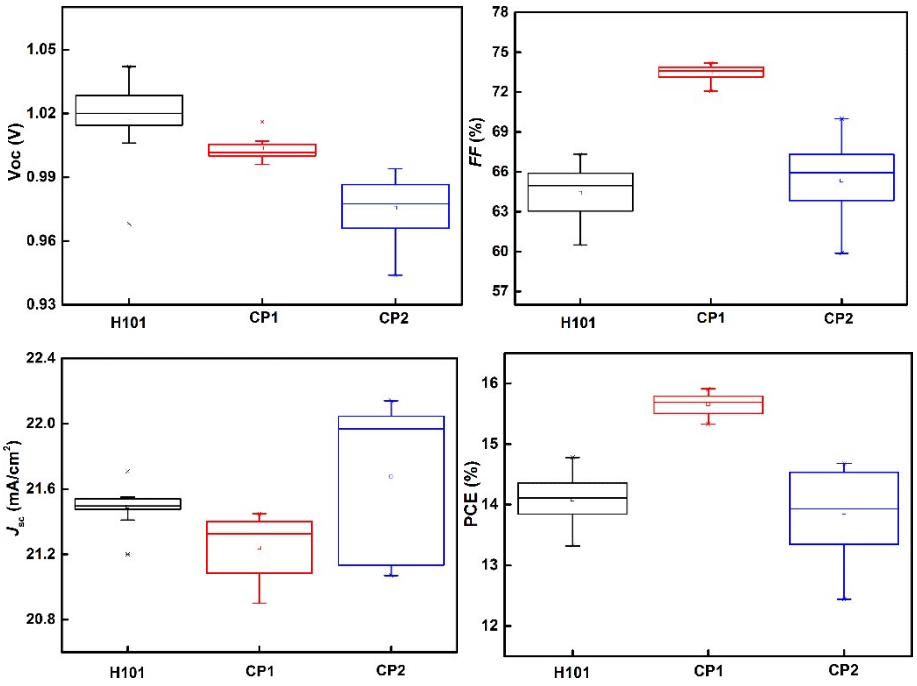

Fig. S10. Box charts of the photovoltaic parameters of the optimal devices based on H101, CP1 and CP2.

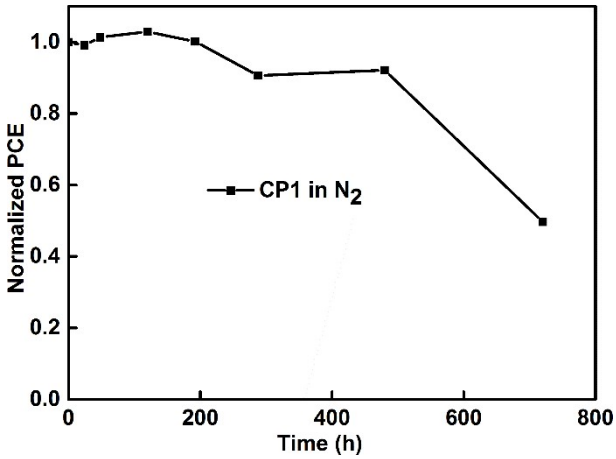

Fig. S11. Stability test of PSCs for CP1 as HTM under room temperature in the dark. The solar cells are stored in a box with a relative humidity of 10% filled with the air gas.

Table S1. The HOMO and the LUMO values obtained with HSE, B3P86, B3LYP, BMK and PBE0 methods (6-311G** basis set was used) of H01 and CP1-CP2.

		HSE [c]	B3P86 [c]	B3LYP [c]	BMK [c]	PBE0 [c]	H101(exp)
H101	HOMO/eV	-4.53	-5.07	-4.67	-5.09	-4.77	-5.18 [a], -5.16 [b]
	LUMO/eV	-2.08	-2.37	-1.92	-1.48	-1.83	-2.48 [a]
CP1	HOMO/eV	-4.99	-5.30	-5.11	-5.54	-5.23	
	LUMO/eV	-2.41	-2.58	-2.24	-1.81	-2.17	
CP2	HOMO/eV	-5.02	-5.33	-5.14	-5.57	-5.26	
	LUMO/eV	-2.45	-2.65	-2.29	-1.87	-2.21	

[a]from ref.[26]

[b]from ref.[27]

[c]The HOMO and LUMO energy calculated by B3P86/6-311G(d,p) is fitted according to the formula:[28]

$HOMO(\text{exp.})=0.66HOMO(\text{th.})-1.75 \quad R=0.79$

$LUMO(\text{exp.})=0.69LUMO(\text{th.})-1.07 \quad R=0.88$

Table S2 Predicted crystal data of investigated molecules.

Molecules	Space group	*a*(Å)	*b*(Å)	*c*(Å)	*α*	*β*	*γ*
H101	$P2_12_12_1$	17.27	11.39	26.80	90.00	59.94	90.00
CP1	$P1$	17.58	19.00	18.32	54.87	73.26	37.20
CP2	$P2_1$	9.96	10.71	36.70	90.00	51.20	90.00

Table S3. Summary of device performance of perovskite solar cell adopting different HTMs (H101, CP1 and CP2) at forward and reverse voltage scans.

HTMs		V_{oc}[V]	J_{sc} [mA cm^2]	*FF* [%]	PCE [%]	HI [%]
H101	forward	1.042	21.53	65.87	14.78	9.9
	reverse	1.022	21.55	60.49	13.32	
CP1	forward	1.007	21.45	73.61	15.91	6.8
	reverse	1.009	21.12	69.62	14.83	
CP2	forward	0.986	21.96	67.83	14.68	15.2
	reverse	0.981	21.16	59.88	12.44	

5. References

1. X. R. Liu and X. Liu, *RSC Adv.*, 2019, **9**, 24733-24741.
2. A. Cohen, P. Mori-Sánchez and W. Yang, *Chem. Rev.*, 2012, **112**, 289-320.
3. J. Tomasi, B. Mennucci and R. Cammi, *Chemical reviews*, 2005, **105**, 2999-3094.
4. M. J. Frisch, G. W. Trucks, H. B. Schlegel, G. E. Scuseria, M. A. Robb, J. R. Cheeseman, G. Scalmani, V. Barone and G. A. Petersson, *Fox, "Gaussian 09," Revision A.1, Gaussian, Inc., Wallingford, 2009.*
5. M. Y. Kuo, H. Y. Chen and I. Chao, *Chemistry-A European Journal*, 2007, **13**, 4750-4758.
6. L. Wang, G. Nan, X. Yang, Q. Peng, Q. Li and Z. Shuai, *Chem. Soc. Rev.*, 2010, **39**, 423-434.
7. J. Bisquert, *Phys. Chem. Chem. Phys.*, 2008, **10**, 3175-3194.
8. W. Q. Deng and W. A. Goddard III, *The Journal of Physical Chemistry B*, 2004, **108**, 8614-8621.
9. R. A. Marcus, *Annu. Rev. Phys. Chem.*, 1964, **15**, 155-196.
10. R. A. Marcus, *Angew. Chem. Int. Ed.*, 1993, **32**, 1111-1121.
11. X. W. Yang, L.; Wang, C.; Long, W.; Shuai, Z. , *Chem. Mater.*, 2008, **20**, 3205–3211.
12. X. Yang, Q. Li and Z. Shuai, *Nanotechnology*, 2007, **18**, 424029.
13. C. Wang, F. Wang, X. Yang, Q. Li and Z. Shuai, *Org. Electron.*, 2008, **9**, 635-640.
14. W. Q. Deng, L. Sun, J. D. Huang, S. Chai, S. H. Wen and K. L. Han, *Nat Protoc*, 2015, **10**, 632-642.
15. B. C. Lin, C. P. Cheng and Z. P. M. Lao, *J. Phys. Chem. A*, 2003, **107**, 5241-5251.
16. S.-H. Wen, A. Li, J. Song, W.-Q. Deng, K.-L. Han and W. A. Goddard III, *The Journal of Physical Chemistry B*, 2009, **113**, 8813-8819.
17. K. Senthilkumar, F. Grozema, F. Bickelhaupt and L. Siebbeles, *J. Chem. Phys.*, 2003, **119**, 9809-9817.
18. J. P. Perdew, J. Chevary, S. Vosko, K. A. Jackson, M. R. Pederson, D. Singh and C. Fiolhais, *Physical Review B*, 1992, **46**, 6671.
19. G. t. te Velde, F. M. Bickelhaupt, E. J. Baerends, C. Fonseca Guerra, S. J. van Gisbergen, J. G. Snijders and T. Ziegler, *J. Comput. Chem.*, 2001, **22**, 931-967.
20. C. F. Guerra, J. Snijders, G. Te Velde and E. Baerends, *Theor. Chem. Acc.*, 1998, **99**, 391-403.
21. Y. L. Xu, W. L. Ding and Z. Z. Sun, *Nanoscale*, 2018, **10**, 20329-20338.
22. *Materials Studio, San Diego, CA*, 2005.
23. G. Day, W. Motherwell, H. Ammon, S. Boerrigter, R. Della Valle, E. Venuti, A. Dzyabchenko, J. Dunitz, B. Schweizer and B. Van Eijck, *Acta Crystallographica Section B: Structural Science*, 2005, **61**, 511-527.
24. R. Jin and Y. Chang, *Physical Chemistry Chemical Physics*, 2015, **17**, 2094-2103.
25. W.-J. Chi and Z.-S. Li, *Physical Chemistry Chemical Physics*, 2015, **17**, 5991-5998.
26. P.-Y. Su, Y.-F. Chen, J.-M. Liu, L.-M. Xiao, D.-B. Kuang, M. Mayor and C.-Y. Su, *Electrochimica Acta*, 2016, **209**, 529-540.
27. H. Li, K. Fu, A. Hagfeldt, M. Graetzel, S. G. Mhaisalkar and A. C. Grimsdale, *Angew. Chem.-Int. Edit.*, 2014, **53**, 4085-4088.
28. X. Liu and X. Liu, *RSC Advances*, 2019, **9**, 24733-24741.